PONTIFICIA UNIVERSIDAD CATOLICA DE CHILE
SCHOOL OF ENGINEERING

STRESS CONSTRAINED COMPLIANCE MINIMIZATION BY MEANS OF THE SMALL AMPLITUDE HOMOGENIZATION METHOD

ESTEBAN ARIEL ZEGPI HUNTER

Thesis submitted to the Office of Research and Graduate Studies
in partial fulfillment of the requirements for the degree of
Master of Science in Engineering

Advisor:
SERGIO GUTIÉRREZ CID

Santiago de Chile, October 2012

PONTIFICIA UNIVERSIDAD CATOLICA DE CHILE
SCHOOL OF ENGINEERING

STRESS CONSTRAINED COMPLIANCE MINIMIZATION BY MEANS OF THE SMALL AMPLITUDE HOMOGENIZATION METHOD

ESTEBAN ARIEL ZEGPI HUNTER

Members of the Committee:
SERGIO GUTIÉRREZ CID
ESTEBAN SÁEZ ROBERT
JUAN FELIPE BELTRÁN MORALES
PABLO IRARRÁZAVAL MENA

Thesis submitted to the Office of Research and Graduate Studies
in partial fulfillment of the requirements for the degree of
Master of Science in Engineering

Santiago de Chile, October 2012

Gratefully to my family

ACKNOWLEDGEMENTS

I owe my deepest gratitude to my advisor, Sergio Gutierrez, whose guidance and support enabled me to accomplish this work. Also to my family and friends whose encouragement helped me through this process.

TABLE OF CONTENTS

LIST OF FIGURES

LIST OF TABLES

ABSTRACT

The problem of minimizing the deformation of an element or structure through a better distribution of reinforcement material, is a very relevant problem in many branches of structural and mechanical engineering. However, it is usual for the optimal solutions for these problems to induce stress concentration in the loading or the supporting zone of the structure, which can cause cracking to appear in said zone. We developed a compliance minimization algorithm capable of constraining the average stress in an arbitrary zone of the structure. This work describes how this algorithm addresses the constraint on the stress and the formulations necessary for its implementation. The algorithm achieves a 15% reduction in peak stress while incurring in a compliance increase of less than 4%, when stress is constrained in the loading zone. Whereas, it achieves up to a 45% reduction in peak stress while incurring in a compliance increase of less than 4%, when stress is constrained in the supporting zone. The possibility of including a pointwise stress constraint is to be explored.

Keywords: Structural Optimization, Homogenization, Stress Concentration, Relaxation.

RESUMEN

El problema de minimizar la deformación de un elemento o una estructura a través de una mejor distribución del material de refuerzo es muy relevante en muchas ramas de la ingeniería estructural y mecánica. Sin embargo, es usual que las soluciones óptimas para este problema presenten concentración de tensiones en la zona cargada o en la zona apoyada de la estructura. Se propone un método de minimización de cumplimiento capaz de restringir la tensión promedio en una zona arbitraria de la estructura. Este trabajo describe como este algoritmo maneja la restricción sobre la tensión y la formulación necesaria para su implementación. Actualmente, el método propuesto logra reducciones del máximo de la tensión de hasta 45% incurriendo en una perdida de cumplimiento inferior al 4%. La posibilidad de incluir restricciones puntuales a la tensión queda por explorar.

Palabras Claves: Optimización Estructural, Homogeneización, Concentración de tensiones, Relajación.

1. INTRODUCTION

Reducing the deformation of a reinforced structure through a better distribution of the reinforcing material is a very important problem in several fields of engineering and mechanics, and has been thoroughly studied by several authors (see, for instance, Allaire (2002), Bendsøe and Sigmund (2003)). The usual approach is to minimize the work done by the external forces, the so-called “compliance”. However, in many cases these solutions induce stress concentration in the loading or supporting zones. This situation is highly undesirable, because these stress “peaks” can cause cracks to appear when the load increases. Therefore it is interesting to develop methods that minimize compliance, but limit stress concentration. In this paper we consider such problem under the perspective of the small amplitude homogenization method introduced in Allaire and Gutierrez (2007). This technique allows us to compute a second order asymptotic expansion in the contrast parameter, of the effective elasticity tensor produced by a volume distribution of reinforcement and a given microstructure. Then we can compute an approximation of both compliance and stress for these variables and then select the optimal microstructure, which turns out to be always a rank-one laminate, and then optimize only on the volume distribution.

The numerical results we present here are restricted to the short cantilever problem for several reason: first because it is a well known problem for minimum compliance, second and most importantly, because we present results for different contrast values and try to reduce the peak values of stress, for which we are only partially successful. The main conclusion of the numerical examples is that the method is indeed able to find configurations that control stress concentration, paying a small price in terms of increases in compliance.

The same or closely related problems have been considered by several authors under different perspectives. Duysinx and Bendsøe, see Duysinx and Bendsøe (1998), studied this problem under the ”Solid Isotropic Material with Penalization” (SIMP) perspective.

Bruggi, see Bruggi (2008), considered the problem of minimum weight under stress constraint, also using SIMP. This work also has a very nice introduction, giving a broad perspective on the state of art. Lipton, see Lipton (2002) or Lipton and Stuebner (2006), studied the problem of maximizing the stiffness of shafts under torsion and constraints on stresses. This allows him to consider the interplay between macro and micro stresses, by using either correctors or stress modulation functions.

A different, but related problem is to minimize stress and completely forget about compliance. This was studied using partial relaxation by homogenization by Allaire, Jouve and Maillot, see Allaire et al. (2008). They considered microstructures produced by sequential laminates of arbitrary finite order and then, using correctors, compute a so-called stress amplification factor that they use as a measure of the total stress. Finally, Kočvara and Stingl see Kočvara and Stingl (2008), considered the minimum weight problem under stress constraints, but in the free material optimization framework.

2. MODEL AND ALGORITHM

2.1. Small Amplitude Aproximation

Let $\Omega \subset \mathbb{R}^2$ be the region under consideration, which represents the structure whose stiffness is to be maximized. Ω is bounded with boundary $\partial\Omega$ being piecewise smooth. We denote by x a generic point in Ω. In general we omit the argument of all functions, unless we want to emphasize some dependence on the position. Let $\chi : \Omega \to \{0, 1\}$ be a characteristic function that takes value 1 if the point x is occupied by the softer material and 0 otherwise.

Then, if we relate through a negative real number η the stiffness of the two materials considered and $\mathbb{C}^0$ is the elasticity tensor of the stiffer material, we can write the elasticity tensor as

$$\mathbb{C}(x) = \mathbb{C}^0 \left(1 + \eta\chi(x)\right)$$

As we can see, η can take any value in $(-1, 0)$, however, since the assumption of small amplitude is being made, this value should be small, i.e. $|\eta| \ll 1$, this restriction, however, renders the method less interesting, as both materials are then not too different. In the section devoted to numerical results we use $\eta = -0.5$, meaning that the reinforcement will be twice as stiff as the matrix, hinting that one can somewhat push a little the restriction on η.

Considering the boundary $\partial\Omega$ divided in two disjoint portions, Γ_D, the portion with Dirichlet boundary condition and Γ_N, the portion with Neumann boundary condition, we can write the following linear elasticity problem

$$\left.\begin{array}{rcll} -div(\mathbb{C}\, e(u)) & = & f & \text{in } \Omega \\ u & = & 0 & \text{on } \Gamma_D \\ \mathbb{C}\, e(u) n & = & g & \text{on } \Gamma_N, \end{array}\right\} \tag{2.1}$$

where, as usual, $e(u) = \frac{1}{2}\left(\nabla u + (\nabla u)^{\mathrm{T}}\right)$ denotes the strain tensor. Furthermore, f denotes the body forces to which the structure is subjected to and g denotes the boundary forces, both are assumed to be known. Then, trying to be quite general, we wish to minimize an objective function of the form

$$J(\chi) = \int\limits_{\Omega} j_1(u)\,dx + \int\limits_{\Gamma_N} j_2(u)\,ds. \tag{2.2}$$

possibly subject to a restriction on the volume of the materials, for example

$$\int\limits_{\Omega} \chi\,dx = \Theta, \tag{2.3}$$

where Θ is the total volume occupied by the softer material and which is prescribed beforehand.

Then, we want to solve

$$\min_{\chi \in \mathcal{U}_{ad}} J(\chi),$$

were $\mathcal{U}_{ad}$ corresponds to the set of all admissible designs, namely

$$\mathcal{U}_{ad} = \left\{ \chi \in L^{\infty}(\Omega; \{0,1\}) \text{ s.t. } \int_{\Omega} \chi\,dx = \Theta \right\}.$$

However, as it has been amply reported in the specialized literature, this problem is generally ill-possed, namely minimizing sequences tend to have finer and finer oscillations. See for example Allaire (2002) and the references therein.

Using the assumption of small amplitude stated before, we perform a second order asymptotic expansion of u with respect to η and about $\eta = 0$, as is usual in small amplitude methods, to have that

$$u = u^0 + \eta u^1 + \eta^2 u^2 + O(\eta^3).$$

Replacing this in problem (2.1) and denoting $\sigma(u^i) = \mathbb{C}^0\, e(u^i)$, yields three problems for u^0, u^1, and u^2, respectively.

$$\left.\begin{array}{rcll} -div\sigma(u^0) & = & f & \text{in } \Omega \\ u^0 & = & 0 & \text{on } \Gamma_D \\ \sigma(u^0)n & = & g & \text{on } \Gamma_N \end{array}\right\} \tag{2.4}$$

$$\left.\begin{array}{rcll} -div\sigma(u^1) & = & div(\chi\sigma(u^0)) & \text{in } \Omega \\ u^1 & = & 0 & \text{on } \Gamma_D \\ \sigma(u^1)n & = & -\chi\sigma(u^0)n & \text{on } \Gamma_N \end{array}\right\} \tag{2.5}$$

$$\left.\begin{array}{rcll} -div\sigma(u^2) & = & div(\chi\sigma(u^1)) & \text{in } \Omega \\ u^2 & = & 0 & \text{on } \Gamma_D \\ \sigma(u^2)n & = & -\chi\sigma(u^1)n & \text{on } \Gamma_N \end{array}\right\} \tag{2.6}$$

It can be seen that u^0 does not depends on χ and therefore, it needs to be calculated only once.

Next, we perform a Taylor expansion of the objective function, which yields

$$\begin{aligned} J(\chi) = \quad & \int_\Omega j_1(u^0)\, dx + \eta \int_\Omega j_1'(u^0)u^1\, dx \\ & + \eta^2 \int_\Omega \left(j_1'(u^0)u^2 + \frac{1}{2} j_1''(u^0)(u^1)^2 \right) dx + \int_{\Gamma_N} j_2(u^0)\, ds \\ & + \eta \int_{\Gamma_N} j_2'(u^0)u^1\, ds + \eta^2 \int_{\Gamma_N} \left(j_2'(u^0)u^2 + \frac{1}{2} j_2''(u^0)(u^1)^2 \right) ds + O(\eta^3). \end{aligned}$$

Using again the concept of small amplitude and neglecting the error term we define

$$
\begin{aligned}
J_{sa}(\chi) = \quad & \int_{\Omega} j_1(u^0)\,dx + \eta \int_{\Omega} j_1'(u^0)u^1\,dx \\
& + \eta^2 \int_{\Omega} \left(j_1'(u^0)u^2 + \frac{1}{2} j_1''(u^0)(u^1)^2 \right)\,dx + \int_{\Gamma_N} j_2(u^0)\,ds \\
& + \eta \int_{\Gamma_N} j_2'(u^0)u^1\,ds + \eta^2 \int_{\Gamma_N} \left(j_2'(u^0)u^2 + \frac{1}{2} j_2''(u^0)(u^1)^2 \right)\,ds
\end{aligned}
$$

Now we would like to calculate a gradient for this function and use it in a minimization algorithm. However, this presents some difficulties, since the function χ only takes the values 0 or 1 and therefore one cannot make arbitrary small perturbations of it. In order to overcome this, one possibility is to relax the problem, in the sense of allowing fine mixtures to appear. These mixtures will be eliminated afterwards, because of their very high cost.

In order to accomplish this, and following the line of the work in Allaire and Gutierrez (2007), we will use the concept of H-measures introduced by Tartar in Tartar (1990). The general idea in the process of relaxation is to consider a sequence of characteristic function χ_n and pass to the limit in the objective function $J_{sa}(\chi_n)$. Due to the weak-$\star$ compactness of $L^\infty(\Omega;\{0,1\})$, we can extract a subsequence that converges to a limit density θ in L^∞ weak-$\star$. We will denote by u^0, u_n^1, u_n^2 the solutions to the problems associated to such subsequence of χ_n. Using this notation and passing to the limit as stated before, we find that u_1^n converges weakly in $H^1(\Omega)$ to u^1, which is the solution to

$$
\left.
\begin{aligned}
-div\sigma(u^1) &= div(\theta\sigma(u^0)) && \text{in } \Omega \\
u^1 &= 0 && \text{on } \Gamma_D \\
\sigma(u^1)n &= \theta\sigma(u^0)n && \text{on } \Gamma_N
\end{aligned}
\right\}
$$

Similarly, we get that u_n^2 converges weakly in $H^1(\Omega)$ to u^2, which now corresponds to the solution to

$$\left.\begin{aligned} -div\sigma(u^2) &= div(\theta\sigma(u^1)) - div(\theta(1-\theta)\mathbb{C}^0 M\sigma(u^0)) && \text{in } \Omega \\ u^2 &= 0 && \text{on } \Gamma_D \\ \sigma(u^2)n &= -\theta\sigma(u^1)n + \theta(1-\theta)\mathbb{C}^0 M\sigma(u^0)n && \text{on } \Gamma_N \end{aligned}\right\} \qquad (2.7)$$

In this problem the second terms of both, the right hand side of the differential equation and of the Neumann boundary condition, come from passing to the limit of $\chi_n e(u_n^1)$ by means of H-measures. From (2.5) we know that $e(u_n^1)$ depends linearly on χ_n through a pseudo differential operator of order 0, with symbol

$$q(x,\xi) = -\frac{\sigma^0\xi \otimes \xi + \xi \otimes \sigma^0\xi}{2\mu|\xi|^2} + \frac{(\mu+\lambda)(\sigma^0\xi \cdot \xi)\xi \otimes \xi}{\mu(2\mu+\lambda)|\xi|^4} \qquad (2.8)$$

This computation is a result from the Hashin-Shtrikman variational principle (see Allaire (2002))and, as usual, λ and μ denote the Lamé parameters and $\otimes$ is the tensor product, then, denoting by $\theta(1-\theta)\nu(dx, d\xi)$ the H-measure of the weak-$\star$ $\theta(1-\theta)\nu(dx, d\xi)$ the H-measure of the weak-$\star$ convergent subsequence of χ_n, we get that

$$\begin{aligned} \lim_{n\to+\infty} \int_\Omega \chi_n \mathbb{C}^0 e(u_n^1) : e(\phi)dx &= \int_\Omega \theta\mathbb{C}^0 e(u^1) : e(\phi)dx \\ &- \int_\Omega \int_{\mathbb{S}_{N-1}} \theta(1-\theta) f_{\mathbb{C}^0}(\xi)\sigma^0 : \mathbb{C}^0 e(\phi)\nu(dx, d\xi). \end{aligned}$$

In this expression, $f_{\mathbb{C}^0}(\xi)$ is a fourth-order tensor that, for any pair of symmetric matrices A and B, is defined by

$$f_{\mathbb{C}^0}(\xi)A : B = \frac{A\xi \cdot B\xi}{\mu} - \frac{(\mu+\lambda)(A\xi \cdot \xi)(B\xi \cdot \xi)}{\mu(2\mu+\lambda)} \qquad (2.9)$$

Finally, the term M corresponds to a fourth-order tensor $M(x)$ defined, for any pair of symmetric matrices A and B, as

$$MA : B = \int_{\mathbb{S}^{N}-1} f_{\mathbb{C}^0}(\xi)A : B\,\nu(x, d\xi). \qquad (2.10)$$

The expression $\mathbb{C}^0 M\sigma(u^0)$ corresponds to the effect of the microgeometry that appears when the problem is relaxed. Due to the fact that we can first minimize on ν, independently of θ, at every $x \in \Omega$ we choose ξ^* as the minimizer of expression (2.9) for $A = \sigma(u^0)$ and $B = \mathbb{C}^0 e(p^0)$, with p^0 the solution of the following first adjoint problem

$$\left.\begin{aligned} -div(\mathbb{C}^0 e(p^0)) &= j_1'(u^0) && \text{in } \Omega \\ p^0 &= 0 && \text{on } \Gamma_D \\ \mathbb{C}^0 e(p^0) n &= j_2'(u^0) && \text{on } \Gamma_N \end{aligned}\right\}$$

The unitary vector ξ^* is plugged into (2.10), yielding $M^\star$. Now we can write the objective function as

$$\begin{aligned} J^*_{sa}(\theta) \;&= \int_\Omega j_1(u^0)\,dx + \int_{\Gamma_N} j_2(u^0)\,ds - \eta \int_\Omega \theta\, \mathbb{C}^0 e(u^0) : e(p^0)\,dx \\ &+ \frac{1}{2}\eta^2 \int_\Omega j_1''(u^0)u^1 \cdot u^1\,dx + \frac{1}{2}\eta^2 \int_{\Gamma_N} j_2''(u^0)u^1 \cdot u^1\,ds \\ &- \eta^2 \int_\Omega \theta\, \mathbb{C}^0 e(u^1) : e(p^0)\,dx + \eta^2 \int_\Omega \theta(1-\theta)\, \mathbb{C}^0 M^\star \sigma(u^0) : e(p^0)\,dx \end{aligned}$$

Finally, the gradient we want to compute can be obtained by taking the derivative of J^*_{sa} with respect to θ, this gradient, evaluated in an arbitrary direction $s \in L^\infty$ corresponds to

$$\begin{aligned} \frac{\partial J^*_{sa}}{\partial \theta}(s) = \;& -\eta \int_\Omega s\sigma(u^0) : e(p^0)\,dx - \eta^2 \int_\Omega s\sigma(u^1) : e(p^0)\,dx \\ & + \eta^2 \int_\Omega s(1-2\theta) M^\star \sigma(u^0) : \mathbb{C}^0 e(p^0)\,dx \\ & - \eta^2 \int_\Omega s\sigma(u^0) : e(p^1)\,dx \end{aligned} \tag{2.11}$$

Here, p^1 is the solution to the following second adjoint problem

$$\left.\begin{aligned} -div(\mathbb{C}^0 e(p^1)) &= j_1''(u^0)u^1 + div(\theta\mathbb{C}^0 e(p^0)) && \text{in } \Omega \\ p^1 &= 0 && \text{on } \Gamma_D \\ \mathbb{C}^0 e(p^0)n &= j_2''(u^0)u^1 - \theta\mathbb{C}^0 e(p^0)n && \text{on } \Gamma_N \end{aligned}\right\}$$

Finally, we must choose the objective functions j_1 and j_2 that we wish to study. Since the problem we are concerned with consists in maximizing the stiffness of the member in consideration, the function j_2 is taken as the compliance of the external force, which correspond to the work performed by the external force on the structure, this is written simply as

$$j_2(u) = g \cdot u \tag{2.12}$$

While solving this problem we will neglect the effects of the structure self-weight and all body forces, hence $j_1(u) = 0$.

Now we have a well defined method to minimize the compliance of the element being considered, but we want to take into account the effect of the stress on the structure, and to accomplish this we consider a functional of the stress given by

$$K(\chi) = \int_\Omega k(\sigma(u))\, dx \tag{2.13}$$

It is important to remark here that k is a smooth function and u should in principle be the solution to (2.1) that, as before, is approximated by the same Taylor expansion used above. We now need to perform the same computations over this function as those we performed previously over the objective function for the compliance. As the procedure is relatively similar, we shall note only the results and the most significant steps.

We can write the expression K_{sa} as

$$\begin{aligned} K_{sa}(\chi) &= \int_\Omega k(\sigma(u^0))\,dx + \eta \int_\Omega k'(\sigma(u^0)) : (\sigma(u^1) + \chi\sigma(u^0))\,dx \\ &+ \frac{\eta^2}{2}\int_\Omega k''(\sigma(u^0))(\sigma(u^1) + \chi\sigma(u^0)) : (\sigma(u^1) + \chi\sigma(u^0))\,dx \\ &+ \eta^2 \int_\Omega k'(\sigma(u^0)) : (\sigma(u^2) + \chi\sigma(u^1))\,dx. \end{aligned} \tag{2.14}$$

As before, u^0, u^1 and u^2 are the solutions of the state equations (2.4), (2.5) and (2.6) respectively. Then, performing a similar procedure as above, we can get the following approximation for this function

$$\begin{aligned} K^*_{sa}(\theta,\nu) &= \int_\Omega k(\sigma(u^0)\,dx + \eta \int_\Omega k'(\sigma(u^0)) : (\sigma(u^1) + \theta\sigma(u^0))\,dx \\ &+ \frac{\eta^2}{2}\int_\Omega (k''(\sigma(u^0))\sigma(u^1)) : \sigma(u^1)\,dx - \eta^2 \int_\Omega \theta\sigma(u^1) : e(q^0)\,dx \\ &+ \frac{\eta^2}{2}\int_\Omega \theta(k''(\sigma(u^0))\sigma(u^0)) : \sigma(u^0)\,dx + \eta^2 \int_\Omega \theta k'(\sigma(u^0)) : \sigma(u^1)\,dx \\ &+ \eta^2 \int_\Omega \theta(k''(\sigma(u^0))\sigma(u^0))\sigma(u^1)\,dx + \eta^2 \int_\Omega \theta(1-\theta) \int_{\mathbb{S}_{N-1}} \tilde{h}(\xi)\nu(dx,d\xi) \end{aligned}$$

In this expression, u_1 is the unique solution to (2.7) and $q^0 \in H^1(\Omega)^2$ is the solution to

$$\left.\begin{aligned} -div(\mathbb{C}^0 e(q^0)) &= -div\,(\mathbb{C}^0 k'(\sigma(u^0))) && \text{in } \Omega \\ q^0 &= 0 && \text{on } \Gamma_D \\ \mathbb{C}^0 e(q^0)n &= (\mathbb{C}^0 k'\,(\sigma(u^0)))\,n && \text{on } \Gamma_N \end{aligned}\right\}$$

The term $\tilde{h}(\xi)$ is given by the following expression

$$\begin{aligned} \tilde{h}(\xi) &= \frac{1}{\mu}\sigma(u^0)\xi \cdot \mathbb{C}^0 e(q^0)\xi - \frac{\mu+\lambda}{\mu(2\mu+\lambda)}(\sigma(u^0)\chi\cdot\xi)(\mathbb{C}^0 e(q^0)\xi\cdot\xi) \\ &+ k'(\sigma(u^0)\mathbb{C}^0 q(x,\xi) + k''(\sigma(u^0))\sigma(u^0) : \mathbb{C}q(x,\xi) \\ &+ \frac{1}{2}\,k''(\sigma(u^0))\mathbb{C}^0 q(x,\xi) : \mathbb{C}^0 q(x,\xi) \end{aligned}$$

Here, $q(x,\xi)$ is still defined by (2.8), and it only depends on the microgeometry.To minimize $K^*_{sa}(\theta)$ we take advantage of the fact that it is linear in ν, so it is enough to take ν as a ν^* in a direction ξ^* which minimizes $\tilde{h}(\xi)$ in $\mathbb{S}^{N-1}$, for the numerical results, we will use the same ξ^* here as the one used for compliance. After the elimination of ν, the objective function $K^*_{sa}(\theta)$ is differentiable with respect to θ. This derivative evaluated in a direction s is given by

$$
\begin{aligned}
\frac{\partial K^*_{sa}}{\partial\theta}(s) \quad &= \eta\int_\Omega sk'(\sigma(u^0)):\sigma(u^0)\,dx - \eta\int_\Omega s\sigma(u^0):e(q^0)\,dx \\
&-\eta^2\int_\Omega s\sigma(u^1):e(q^0)\,dx + \eta^2\int_\Omega sk'(\sigma(u^0)):\sigma(u^1)\,dx \\
&+\eta^2\int_\Omega s(k''(\sigma(u^0))\sigma(u^0)):\sigma(u^1)\,dx \\
&+\frac{\eta^2}{2}\int_\Omega s(k''(\sigma(u^0))\sigma(u^0)):\sigma(u^0)\,dx \\
&+\eta^2\int_\Omega s\sigma(u^0):e(q^1)\,dx + \eta^2\int_\Omega s(1-2\theta)\tilde{h}(\xi^*)\,dx
\end{aligned}
\tag{2.15}
$$

Here, q^1 is the solution in $H^1(\Omega)^N$ to

$$
\left.
\begin{aligned}
-div(\mathbb{C}^0 e(q^1)) \quad &= div(\theta\mathbb{C}^0(-e(q^0)+k'(\sigma(u^0))+k''(\sigma(u^0))\sigma(u^0))) \\
&\quad +div(\mathbb{C}^0 k''(\sigma(u^0))\sigma(u^1)) \qquad \text{in } \Omega \\
q^1 \quad &= 0 \qquad\qquad \text{on } \Gamma_D \\
\mathbb{C}^0 e(q^1)n \quad &= \theta\mathbb{C}^0\big(e(q^0)-k'(\sigma(u^0))-k''(\sigma(u^0))\sigma(u^0)\big)n \\
&\quad -\mathbb{C}^0 k''(\sigma(u^0))\sigma(u^1)n \qquad \text{on } \Gamma_N
\end{aligned}
\right\}
\tag{2.16}
$$

Now we can compute a gradient for the approximated compliance (2.11) and a gradient for the approximated stress (2.15), both in an arbitrary direction s. As usual with constrained optimization, one must choose this direction carefully and because of this difficulty, we decided to use a lagrangian formulation as explained in the next section.

2.2. Algorithm

As stated in the last section, we have the necessary expressions to compute a gradient for the compliance and a gradient for some function K of the stress $\sigma(u)$. We propose a function that considers the integral over a subdomain ω of the element of the norm of the stress to a power $2p$, namely the integrand would be

$$k(\sigma(u)) = \chi_\omega \|\sigma(u)\|^{2p}. \tag{2.17}$$

Therefore ω is the region where we want to control the average stress and is chosen by the designer. The parameter $p \geq 1$ has also to be chosen beforehand by the designer and its purpose is to assign a greater cost to peaks in the stress distribution. The function $\chi_\omega(x)$ is the characteristic function of ω, hence it takes value 1 if the point x is in ω and 0 otherwise.

We consider a Lagrangian formulation to manage the stress constraint, therefore we call

$$\mathcal{L}(\theta, l) = J^*_{sa}(\theta) + l\left(K^*_{sa}(\theta) - T_{max}\right). \tag{2.18}$$

Here l corresponds to the Lagrange multiplier associated to the stress constraint and its value is to be adjusted during the optimization cycle. T_{max} represents the upper bound on the average of $K(\sigma)$ in the region ω and it is also to be chosen by the designer.

The gradients for the compliance and the stress constraint are combined using the same Lagrangian formulation and then, the gradient used in the optimization cycle is of the form

$$\frac{\partial \mathcal{L}}{\partial \theta}(s^*) = \frac{\partial J^*_{sa}}{\partial \theta}(s^*) + l\frac{\partial K^*_{sa}}{\partial \theta}(s^*). \tag{2.19}$$

In this expression, s^* corresponds to the direction of steepest descent for $\frac{\partial \mathcal{L}}{\partial \theta}$. In order to be able to compute the value of the gradient, we need to know the value of θ beforehand, for this we must choose a starting distribution, a homogeneous initial distribution (i.e. $\theta = \theta_0$) was chosen.

Now we can write the general optimization procedure that we use:

1. Let Θ, η, E and ν be known quantities that represent the properties of the stiffer material, let also g be a function that represents the external forces that act on Γ_N.
2. Let θ_0 be an arbitrary initial distribution for the material and l_0 and initial value for the Lagrange multiplier.
3. Using θ_0 compute u^0, p^0 and q^0, these values do not change with respect to θ, therefore this step is done only once.
4. Using θ_0 compute u^1, p^1 and q^1.
5. Compute $\mathcal{L}(\theta_0, l_0)$.
6. Compute $\frac{\partial \mathcal{L}}{\partial \theta}(s^*)$.
7. For a value of the stepsize $t > 0$ we update the value of θ by $\theta = \theta_0 + t\frac{\partial \mathcal{L}}{\partial \theta}(s^*)$, restricting θ such that $\theta \in [0, 1]$ and it satisfies the volume constrain.
8. We compute a new value for u^1 and use it to evaluate $\mathcal{L}(\theta, l)$.
9. If the averaged stress in ω is greater than T_{max}, the value of the Lagrange multiplier l is increased, otherwise, l is decreased.
10. i) If $\mathcal{L}(\theta, l) < \mathcal{L}(\theta_0, l_0)$, the values of p^1 and q^1 are recomputed, the assignments $\theta_0 = \theta$ and $l_0 = l$ are made and we return to step (6).

    ii) If $\mathcal{L}(\theta, l) \geq \mathcal{L}(\theta_0, l_0)$, the magnitude of t is reduced and we return to step (7).
11. The method stops if t becomes smaller than an arbitrary value t_{min} or if the number of iterations reaches a predefined value.

This algorithm was implemented in the finite element package FreeFEM++ (see Hecht et al. (2007)).

3. NUMERICAL RESULTS

The algorithm just described was implemented to solve a typical problem in structural optimization, namely the short cantilever, which has been studied by various authors (see, for instance, Bendsøe and Sigmund (2003)). It consists of a tall short beam subjected to a vertical load applied in the middle of the right vertical side and fixed on the opposite side. Both horizontal sides are left free. This problem is usually solved for a domain of height twice its width, however, we change the usual domain, using instead $\Omega = (0,1) \times (-0.2, 2.2)$, with dimensions in meters, and fixing the left vertical side only in the interval $(0,2)$, because the results obtained using small amplitude homogenization for compliance minimization, see Allaire and Gutierrez (2007), showed a slight tendency to try to escape the usual domain. See the physical setting in figure 3.1, where we also show the subsets where the stress will be constrained. The subsets ω_1 and ω_2 are described by

$$\begin{aligned}\omega_1 = \; & \{(x,y) \in \mathbb{R}^2 \text{ s.t. } x \in [0,1] \\ & \text{and } (x-1.15)^2 + (y-1)^2 < 0.225^2\}\end{aligned}$$

$$\begin{aligned}\omega_2 = \; & \{(x,y) \in \mathbb{R}^2 \text{ s.t. } x \in [0,1] \\ & \text{and } (x+0.04)^2 + y^2 < 0.13^2 \\ & \text{or } (x+0.04)^2 + (y-2)^2 < 0.13^2\} \,.\end{aligned}$$

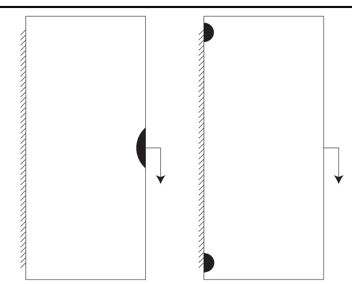

Figure 3.1: Diagram of the physical setting and zones where the stress is constrained marked in black: ω_1 (left) and ω_2 (right).

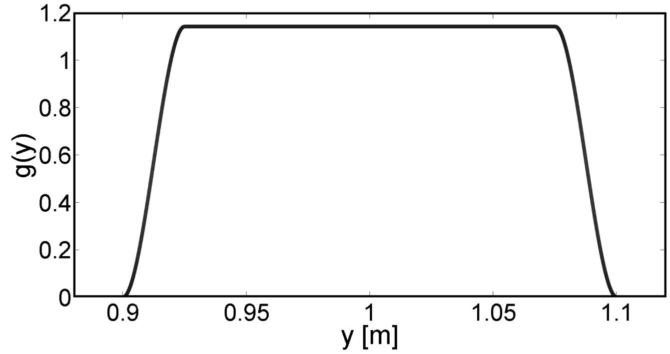

Figure 3.2: Diagram of the load function applied in Γ_N

The elastic parameters for the reinforcement in the following examples are: $E = 1\,\frac{kgf}{cm^2}$ and $\nu = 0.33$. The area covered by reinforcement is $0.528\,m^2$, then, since the total area is $2.4\,m^2$, the matrix area is $\Theta = 1.872\,m^2$, that corresponds to 78% of the total area. The contrast parameter is $\eta = -0.5$.

Since we are interested in the stress and its peaks, the usual constant load function is not suitable as it induces concentrations of stress on the edges of the zone where it is applied. Hence we propose instead to use a slightly different load function, which is shown in figure 3.2. This load function is such that near the edges of the loading zone its extremes are cubic functions over intervals of length $0.025\,m$ and whose value and first derivatives vanish at the edges of the loading zone, and it is locally constant everywhere else.

The problem was solved by means of triangular discretizations with approximately 30,000 triangles. When comparing results, exactly the same mesh is used in all cases. In order to get classical results we use a penalization method. The interest of having classical shapes is twofold: first, classical solutions are much cheaper to construct; secondly, we want to evaluate directly the stress in the proposed configurations, without recourse to an approximation of the effective elasticity tensor being used at each point, in order to have a more accurate comparison of the quality of the configurations we propose. Therefore in the following results, we compute the optimal reinforcement distributions using the algorithm proposed in the previous section, then we penalize this distribution to get a classical configuration, over which we recompute both the compliance and the stress field, from which we obtain the numbers shown in the tables.

The solution for compliance minimization in this physical setting and high stiffness contrast between the matrix and the reinforcement, the so-called large amplitude case, is well known and can be obtained using Full Homogenization (F.H.). It consists of two 90° bars, and it is presented in figure 3.3 a). In figure 3.3 b) we present the stress distribution in this configuration calculated for $\eta = -0.5$, which highly concentrates stress around the loading zone and the edges of the supporting zone, which justifies the election of regions ω_1 and ω_2 shown in figure 3.1. To further clarify this point, in 3.3 c) we zoom in to the loading zone, to show that the stress actually concentrate in a smaller set, since it has two large peaks. Even though this large amplitude problem is the one engineers would like to solve, there is no mathematical framework to solve it yet constraining stress. Hence, as an incremental step, we study the case when the contrast is 50%. First, using the Small Amplitude Homogenization (S.A.H.) method proposed in Allaire and Gutierrez (2007), we can obtain the configuration that minimizes compliance, which can be seen in figure 3.4 a). As before, we also show the stress distribution and zoom in to the problematic region in figures 3.4 b) and 3.4 c), respectively. We can see that the stress peaks are even higher than in the configuration computed for large amplitude.

We will use these known solutions, specially the second one, as references, or benchmarks, to assess the performance of the method proposed in this work.

3.1. Stress constrained in the loading zone

First we use $p = 2$ in the stress constraint, and constrain $K^*_{sa}(\theta)$ to be below $T_{max} = 0.04411$, which is the most stringent value for which the method converges. Then penalizing we get the classical solution shown in 3.5 a), the stress distribution and

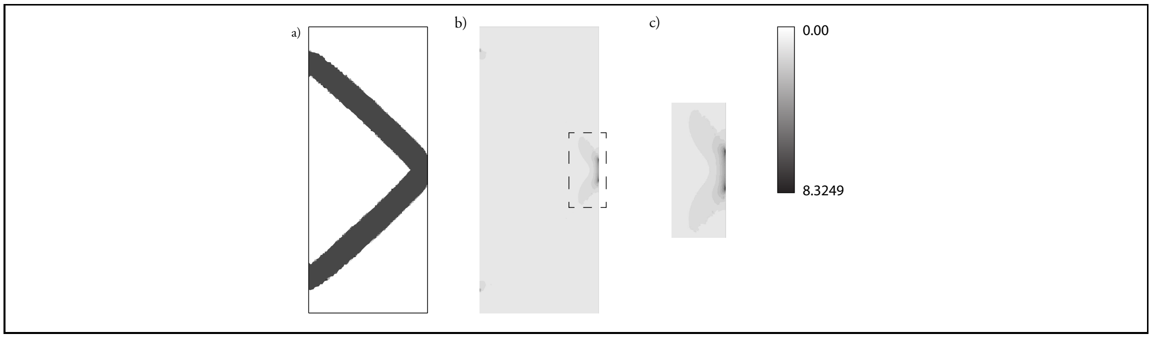

Figure 3.3: a) Optimal solution for compliance minimization using Full Homogenization for large contrast, b) Stress distribution using $\eta = -0.5$, c) Zoom around the loading zone.

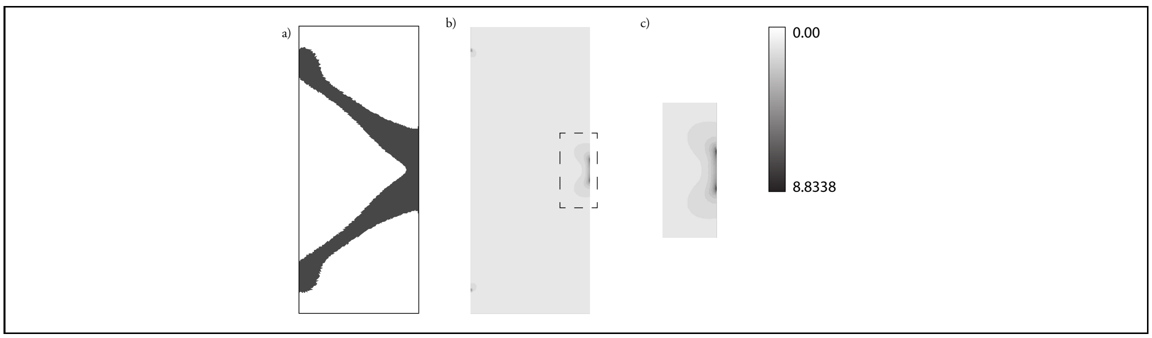

Figure 3.4: a) Optimal solution for compliance minimization using Small Amplitude Homogenization, b) Stress distribution, c) Zoom around the loading zone.

zoom in to the zone of ω_1 are shown in figures 3.5 b) and 3.5 c). Then we would like to compare this with the reference configurations mentioned in the previous paragraph. Since we have three classical solutions, we can evaluate $K(\chi)$ exactly. We need to keep in mind that during the optimization $K(\chi)$ is approximated by $K^*_{sa}(\theta)$, which is restricted to be below T_{max}. Hence if we make T_{max} progressively smaller and if we are still able to find a solution that satisfies this constraint, we are forced to get at convergence a higher value for the compliance, because we are then solving a more restricted problem. This is clearly seen in table 3.1. More important is that the increase in compliance is less than 4% compared to the solution just for minimal compliance, while the reduction on $K(\chi)$ is about 13%.

Taking the optimal solution using Full Homogenization for minimal compliance shown in figure 3.3a) and computing the square of the norm of the stress on the boundary

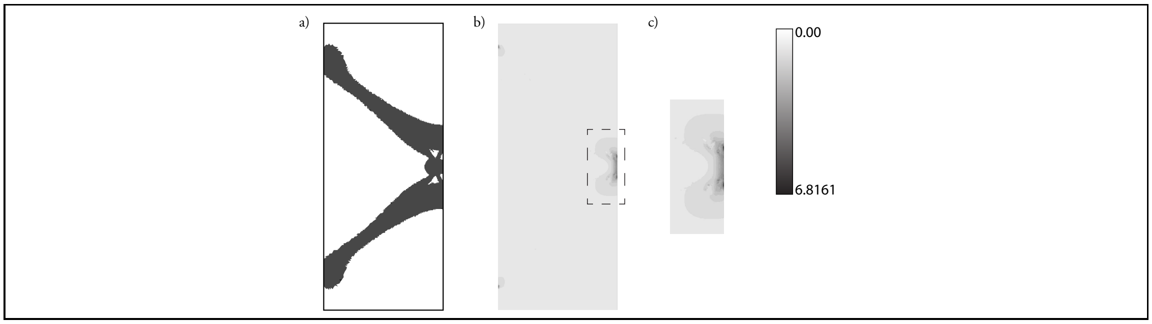

Figure 3.5: a) Optimal solution for compliance minimization using Small Amplitude Homogenization and restricting stress around the loading zone. b) Stress distribution. c) Zoom around the loading zone.

	F.H.	S.A.H.	S.A.H. Rest.	% Var.
Compl.	0.1497	0.1468	0.1529	4.2
$K(\chi)$	0.0453	0.0495	0.0429	-13.3
$\max\|\sigma\|^2$	8.3249	8.8338	6.8161	-22.8

TABLE 3.1. Effect on the compliance and stress when restricting the average stress in ω_1.

of the right side, gives the function shown in figure 3.6 a). Doing the same for the Small Amplitude Homogenization solution shown in figure 3.4a) yields the result shown in figure 3.6 b). We can see in both cases, that there is a large stress concentration near the edges of the loading zone of the boundary. Finally, doing the same for the configuration shown in figure 3.5, we get the function shown in figure 3.6 c). The peak of the square of the norm of the stress is in the latter about 15.5% smaller compared to the first case and 21.4% smaller compared to the second case, and, as it was mentioned above, the increment in compliance is just 4.2%.

However, the highest stress peaks do not appear in the loading boundary itself, instead they appear in close proximity of it. In the third row of table 3.1 we can appreciate the peak value for the cases shown in figures 3.3, 3.4 and 3.5. We see that the reduction is of the same order than that for the boundary, giving a reduction of 16.3% for the first case and 22.8% for the second case.

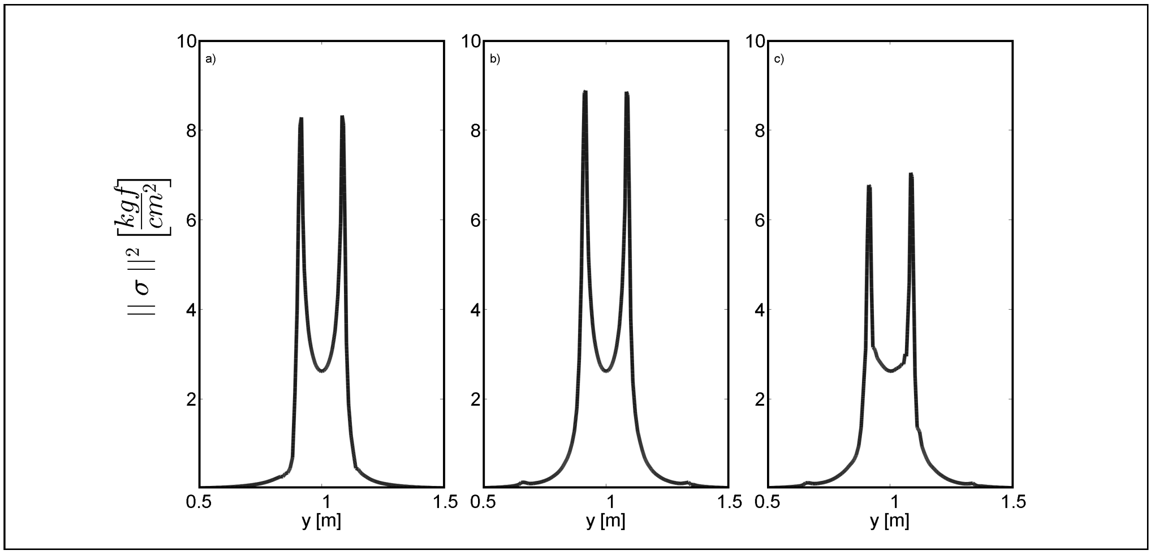

Figure 3.6: a) Stress distribution on the boundary for the Full Homogenization solution. b) Stress distribution on the boundary for the Small Amplitude Homogenization solution. c) Stress distribution on the boundary for the proposed solution.

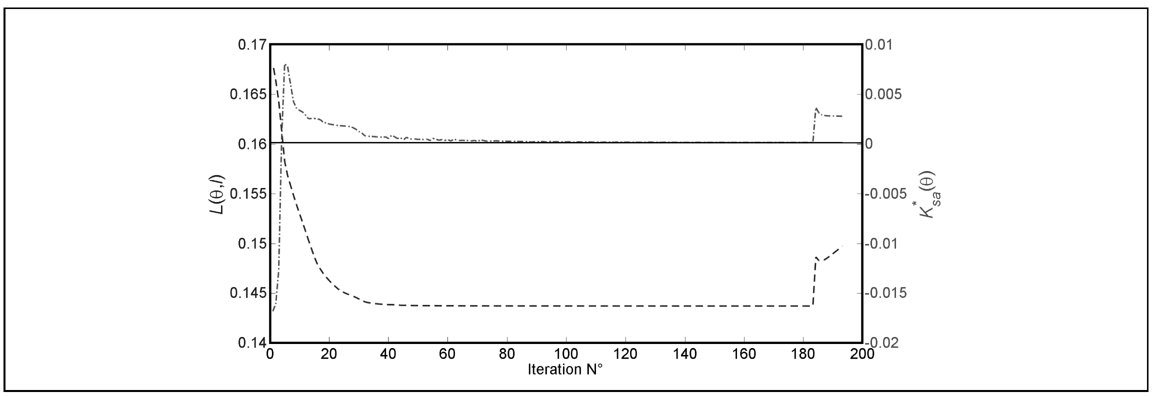

Figure 3.7: Convergence histories for the case subjected to a stress constrain in ω_1.

To showcase the speed of convergence of the method, we display in figure 3.7 the convergence history for the example shown in figure 3.5. As we can see there, the algorithm approaches the optimal value very quickly, in fact, after the 50^{th} iteration the gain from further iterations is very small. Around the 185^{th} iteration we appreciate a sudden increase in the value of the objective function, which corresponds to the beginning of the penalization procedure aimed to obtain classical designs. The convergence history for the compliance in the example of figure 3.4 is very similar, showing that the introduction of a constraint over the stress does not harm the speed of convergence of the algorithm.

3.2. Peak stress reduction by increasing p

Given the peaks in the norm of the stress squared, that appear in figure 3.6 and in the close ups of figures 3.3c), 3.4c) and 3.5c), we try to reduce these peaks by increasing the value of p. Since this makes non-comparable the values of T_{max} being used for each value of p, we decided to take for each case the smallest value of T_{max} that gave convergence of the method. In table 3.2 we can see the value of the peaks in the norm of stress squared, obtained for three different values of p, with the penalized configurations displayed in figure 3.8. We see that increasing the value of p leads to smaller peak values of the norm of the stress squared and higher values of compliance. Comparing the cases $p = 1$ and $p = 2$ we see an increase of 2.2% in compliance, as the price to pay for a peak stress reduction of 17.3%.

	$p = 1$	$p = 1.5$	$p = 2$
Compl.	0.1496	0.1522	0.1529
$max\|\sigma\|^2$	8.2400	8.1503	6.8161

TABLE 3.2. Effect of the parameter p on the stress peak.

In figure 3.8 we see that the distribution of material in the zone in which we want to control the stress varies significantly as we change the value of p. Most notably, we can see that, as the value of p increases, the method moves the stiffer material away from the zones in which stress has peaks (namely the edges of the loaded section of the boundary) and also moves the stiffer material outside of ω_1.

In figures 3.9 and 3.5 we can see the stress distributions for the left and right configurations shown in figure 3.8, respectively. We see from the scale that the values for the stress are lower for configuration on the right in figure 3.8, and, if one looks carefully at the close up figures, it can be noted that the darker area in the case $p = 2$ is both a little longer and a little wider, showing a better stress distribution. If, by comparison, we look at the stress distribution for the unconstrained case in figures 3.4 b) and c), we notice that the stress is more concentrated in the loaded zone and that the value of the

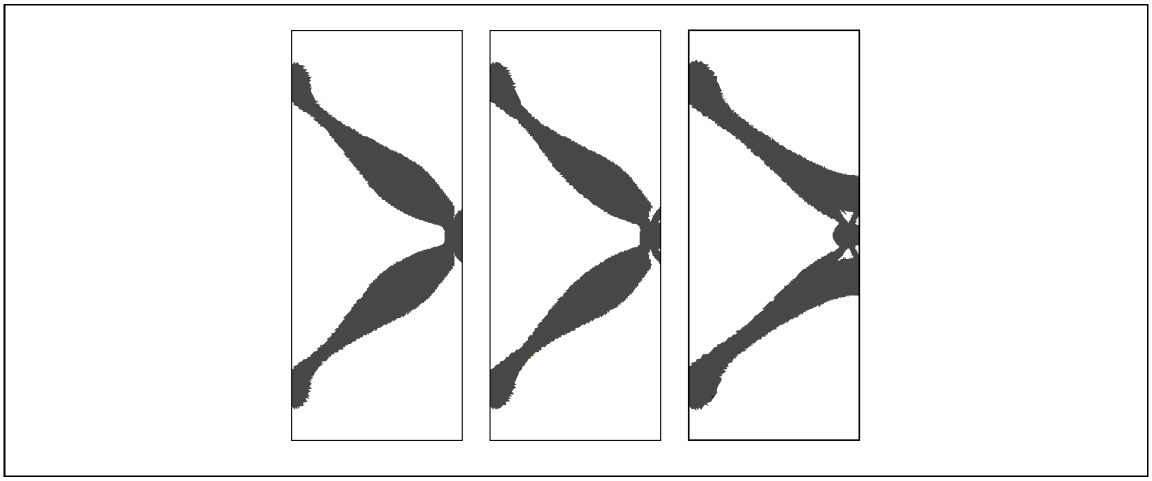

Figure 3.8: Optimal configuration for $p = 1$, $p = 1.5$ and $p = 2$.

peaks are indeed higher, hinting to the success of the proposed method in controlling stress concentration.

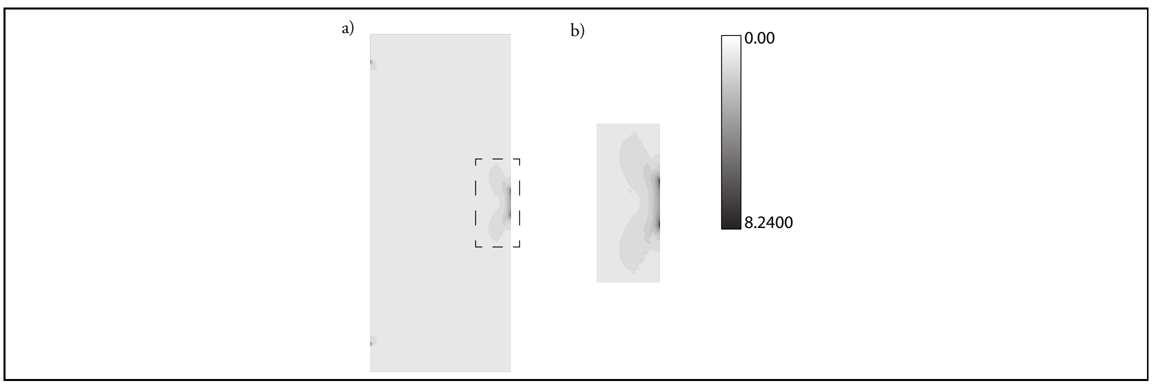

Figure 3.9: a) Stress distribution for $p = 1$. b) Zoom around the loaded zone.

3.3. Stress Constrained on the supporting zone

We have shown that the method works quite well in constraining the stress in the loading zone, while incurring in a small increase in compliance. Now we show the results when constraining the stress in the edges of the supporting zone, namely in ω_2, and using again $p = 2$. The triangular finite elements mesh used in the previous case is modified to make it finer around ω_2, specially near the edges of the supporting zone, instead of ω_1.

As before, we start by comparing in terms of compliance and stress, the benchmark configurations to the solution proposed by our method, which is presented in figure 3.10, where a close up of the upper edge of the supporting zone is also shown, where one can notice that the algorithm leaves a very small hole at the edge of the supporting zone, which is due to the large peak of stress that occurs there. The main difference between the proposed configuration and that of figure 3.4 is that part of the stiffer material is taken away from the edges of the supporting zone, this, as is to be expected, incurs in an increase in compliance, but also results in a reduction of peak in the norm squared of the stress in ω_2.

In table 3.3 we can see the performance of this solution compared to our benchmark cases, both in compliance and in stress, measured by $K(\chi)$ and the peak of $\|\sigma\|^2$ in ω_2. We consider the peak stress only in ω_2, because the overall peak is attained near the loading zone. As expected, compliance is larger for the proposed solution than the compliance for the optimal configuration for minimal compliance, however, the difference is about 1.3%, while the difference in both $K(\chi)$ and peak stress, is about 45%. It is important to notice that the stress peak did not move after optimization, meaning that the proposed solution actually reduces the peak stress and does not simply moves it outside of ω_2.

	F.H.	S.A.H.	S.A.H. Rest.	% Var.
Compl.	0.14451	0.14335	0.14519	1.3
$K(\chi)$	0.00269	0.00351	0.00187	-46.7
$\max_{\omega_2} \|\sigma\|^2$	8.2286	10.5619	5.7522	-45.5

TABLE 3.3. Effect on the compliance and stress in ω_2 when restricting the stress in this set.

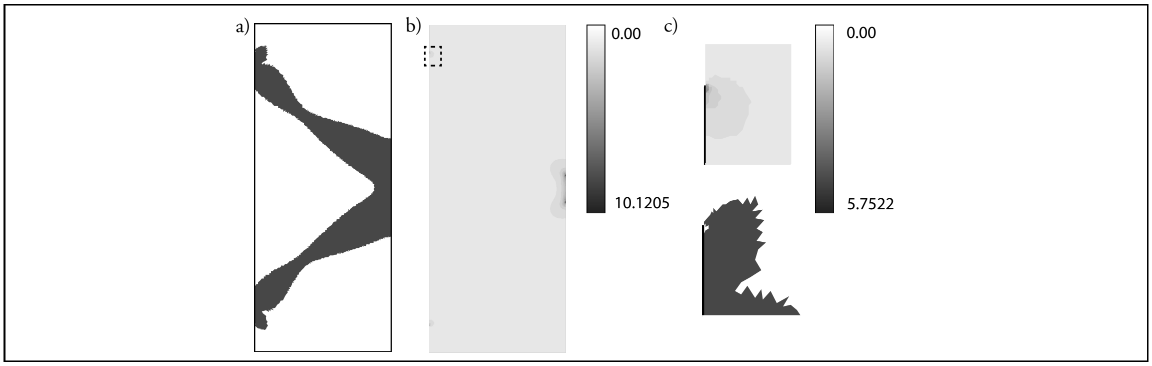

Figure 3.10: a) Optimal solution for small amplitude compliance minimization considering a constraint on stress in ω_2 with $p = 2$. b) Stress distribution using $\eta = -0.5$. c) Zoom around the zone enclosed by the dashed rectangle.

4. CONCLUSIONS

We have shown a method capable of finding the optimal reinforcement distribution for minimizing the compliance of an element while maintaining a function of the stress in a given zone below a certain threshold. Furthermore, the method enables the designer, to an extent, to control the peaks on stress in the specified zone. The increase in compliance is maintained within acceptable limits. Even though the method was implemented in 2-D, there is no additional mathematical difficulty in the 3-D case. There would be, naturally, a significant increase in computational cost associated to using fine meshes in 3-D.

While the method is quite well defined, the numerical considerations and strategies to implement it are not. A dual method for computing stresses might certainly improve their estimation. Also the handling of the Lagrange multiplier l associated to the stress constraint, leads to some difficulties when implementing the method, as the updating scheme of this parameter must be studied on a case-by-case basis.

5. PERSPECTIVES

The term M discussed in the presentation of the method, is chosen as the optimal for compliance minimization, which is certainly not the optimal for stress minimization, therefore, future work could be done in order to include the calculation for the optimal direction of lamination as a compromise between the optimal for compliance and the optimal for the function of the stress. However, as this participates only on part of the corresponding second order terms, it is not clear that this would lead to significant gains in performance.

The possibility of including a way to consider pointwise constraints on the stress is to be explored, as it has been seen that if the zone ω where the average stress is restricted is very small, the algorithm does not perform so well.

Even though the examples above show that it is possible to control the norm of the stress, the inclusion of a physically more meaningful stress measure could also be considered in a similar mathematical and computational framework. For instance, Von Mises or Tresca yield criteria could be used, which would probably lead to more interesting results from an engineering standpoint.

REFERENCES

G. Allaire. *Shape Optimization by the Homogenization Method*. Springer, 2002.

G. Allaire and S. Gutierrez. Optimal design in small amplitude homogenization. *Math. Modelling and Num. Analysis*, 41, 2007.

G. Allaire, F. Jouve, and H. Maillot. Topology optimization for minimum stress design with the homogenization method. *Struct. Multidiscip. Optim.*, 36, 2008.

M.P. Bendsøe and O. Sigmund. *Topology Optimization. Theory, Methods and Applications*. Springer, 2003.

M. Bruggi. On an alternative approach to stress constraints relaxation in topology optimization. *Struct. Multidiscip. Optim.*, 36, 2008.

P. Duysinx and M.P. Bendsøe. Topology optimization of continuum structures with local stress constraints. *International Journal for Numerical Methods in Engineering*, 43, 1998.

F. Hecht, O. Pironneau, A. Le Hyaric, and K. Ohtsuka. *FreeFem++, code and user manual freely available at www.freefem.org*. Laboratoire Jacques-Louis Lions, 2007.

M. Kočvara and M. Stingl. Small amplitude homogenization applied to inverse problems. *J. Comp. Mech.*, 41, 2008.

R. Lipton. Design of functionally graded composite structures in the presence of stress constraints. *Int. J. Solids and Structures*, 39, 2002.

R. Lipton and M. Stuebner. Optimization of composite strutures subject to local stress constraints. *Comp. Meth. in Applied Mech.and Eng.*, 196, 2006.

L. Tartar. H-measures, a new approach for studying homogenization, oscillations and concentration effects in partial differential equations. *Proc. of the Royal Soc. Edinburgh*, 115A, 1990.